CFD modelling of sludge sedimentation in secondary clarifiers

M. Weiss, B. Gy. Plosz, K. Essemiani & J. Meinhold
Anjou Recherche Veolia Water, France

Abstract

We present a CFD model that predicts the sedimentation of activated sludge in a full-scale circular secondary clarifier that is equipped with a suction-lift sludge removal system. The axisymmetric single-phase model is developed using the general-purpose CFD solver FLUENT 6, which uses the finite-volume method. A convection-diffusion equation, which is extended to incorporate the sedimentation of sludge flocs in the field of gravity, governs the mass transfer in the clarifier. The standard k-ε turbulence model is used to compute the turbulent motion, and our CFD model accounts for buoyancy flow and non-Newtonian flow behaviour of the mixed liquor. The activated sludge rheology was measured for varying sludge concentrations and temperatures. These measurements show that at shear rates typical of the flow in secondary clarifiers, the relationship between shear stress and shear rate follows the Casson law. The sludge settling velocity was measured as a function of the concentration, and we have used the double-exponential settling velocity function to describe its dependence on the concentration. The CFD model is validated using measured concentration profiles.
Keywords: computational fluid dynamics, wastewater treatment, activated sludge, secondary clarifiers, sedimentation, rheology, suction-lift sludge removal.

1 Introduction

Secondary clarifiers represent the final stage in the activated sludge wastewater treatment process, separating the treated water from the biologically active sludge (fig. 1). This solid/liquid separation is traditionally achieved by gravity sedimentation. These separation units, which act as clarifier, thickener, and storage tank, are often the major bottlenecks in the activated sludge process. Our

WIT Transactions on Engineering Sciences, Vol 52, © 2006 WIT Press
www.witpress.com, ISSN 1743-3533 (on-line)
doi:10.2495/AFM06050

objective is the development of a modelling tool that may be used in design and optimisation of new and existing secondary clarifiers.

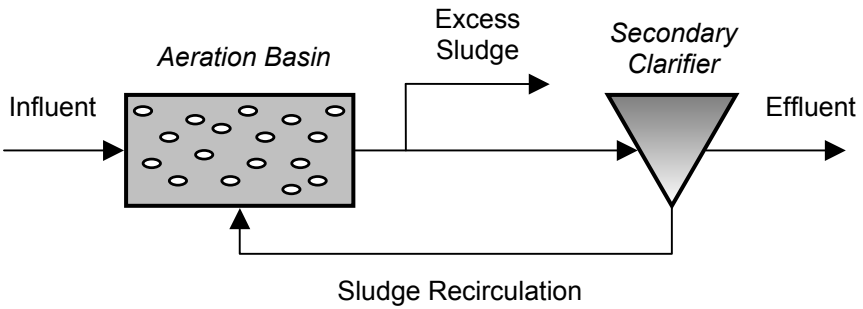

Figure 1: Scheme of an activated sludge wastewater treatment process.

The present study concerns circular clarifiers that are equipped with suction-lift sludge removal systems. In these clarifier systems, which usually have a flat bottom, the sludge is withdrawn through an array of vertical suction pipes from the near-bottom region. This design form may be contrasted with clarifiers that have conical bottoms and where the sludge is removed centrally at the bottom.

We present a computational fluid dynamics (CFD) model of the secondary clarifiers at the wastewater treatment plant of Saint Malo (France), which rests on the numerical model presented by Lakehal *et al*. [1]. Our CFD model differs from that of the aforementioned authors in mainly two ways: (*i*) it employs negative source terms on the governing field equations that represent the sludge removal by suction-lift, and (*ii*) it uses the Casson viscosity law instead of the Bingham law to reflect the non-Newtonian flow behaviour of the activated sludge. We have carried out on-site experiments to determine the rheological flow behaviour and the settling characteristics of the sludge mixture. In addition, the inlet concentration and the flow rates were measured. We have measured concentration profiles within the clarifier to validate the numerical model.

2 Field equations for turbulent flow

The system of Reynolds-averaged flow-governing partial differential equations for two-dimensional, axisymmetric, unsteady, density-stratified, and turbulent mean flow may be given as [1]

$$\frac{\partial u}{\partial x}+\frac{\partial v}{\partial y}+\frac{v}{y}=S_m\,, \tag{1}$$

$$\begin{aligned}\frac{\partial u}{\partial t}+\frac{\partial u^2}{\partial x}+\frac{\partial (uv)}{\partial y}=&-\frac{1}{\rho_w}\frac{\partial p}{\partial x}+\frac{\partial}{\partial x}\left(2(\nu+\nu_t)\frac{\partial u}{\partial x}\right)+\\&+\frac{1}{y}\frac{\partial}{\partial y}\left(y(\nu+\nu_t)\left(\frac{\partial u}{\partial y}+\frac{\partial v}{\partial x}\right)\right)-g\left(\frac{\rho}{\rho_w}-1\right)+S_x\,,\end{aligned} \tag{2}$$

and

$$\frac{\partial v}{\partial t}+\frac{\partial (uv)}{\partial x}+\frac{\partial v^2}{\partial y}=-\frac{1}{\rho_w}\frac{\partial p}{\partial y}+\frac{\partial}{\partial x}\left((\nu+\nu_t)\left(\frac{\partial u}{\partial y}+\frac{\partial v}{\partial x}\right)\right)+ \\ +\frac{1}{y}\frac{\partial}{\partial y}\left(2y(\nu+\nu_t)\frac{\partial u}{\partial y}\right)-\frac{2(\nu+\nu_t)}{y}\frac{v}{y}+S_y. \tag{3}$$

The equation of continuity is given in eqn (1), and eqns (2) and (3) are the x and y momentum conservation equations, respectively. The origin of the coordinate system is placed on the vertical centre line, with the x-axis pointing vertically upwards from the bottom boundary (fig. 2). We note that the field equations are given in terms of averaged flow variables, where u and v are the mean velocity components in the x (axial) and y (radial) directions, respectively, p is the pressure, ρ is the density of the mixed liquor, ρ_w = 998.2 kg m^{-3} is the density of water, g = 9.81 m s^{-2} is the gravitational acceleration constant, ν is the kinematic viscosity of the mixed liquor, and ν_t is the turbulent viscosity.

We have added source terms S_m, S_x, and S_y to eqns (1) to (3) that represent the removal of sludge by suction-lift. These source terms, which are defined as $S_m = -(q_{rec}/V_{rec})$, $S_x = -(q_{rec}/V_{rec})u$, and $S_y = -(q_{rec}/V_{rec})v$, are negative since sludge is removed from the system. They contain the mass flow rate of the recycle stream in [kg s^{-1}], q_{rec}, which is obtained from flow measurements. The volume of the sludge removal zone in the near-bottom region of the clarifier in [m^3], V_{rec}, is defined further down in the paper. The source terms are built into the CFD code using user-defined functions (UDFs) in Fluent.

The governing field equations are formulated using the density of water, and we account for the varying density of the sludge mixture only in the buoyancy terms in the axial momentum equation, eqn (2), and in the equation for the turbulent kinetic energy, eqn (6), which is given further down. We add the buoyancy term to the x momentum equation using a UDF in Fluent. The on-site density measurements of Dahl [2] have shown that the relative density increase at a total suspended solids concentration of 12 kg m^{-3} is only 0.4%. However, the density increases sharply at the sludge blanket, and the buoyancy effect that is caused by this gradient on the flow cannot be neglected.

The density of the mixed liquor, ρ, in the buoyancy term of the x momentum equation may be expressed using an equation of state,

$$\rho = \rho_w + X\left(1-\frac{\rho_w}{\rho_p}\right), \tag{4}$$

where ρ_p = 1600 kg m^{-3} is the density of dry sludge particles [2,3], and X is the sludge concentration, which has the same units as the density.

3 Standard k-ε turbulence model

The turbulent (or eddy) viscosity, $\nu_t = \mu_t/\rho_w$, is determined by the turbulent kinetic energy, k, and also by the rate of dissipation of turbulent kinetic energy, ε, according to [1]

$$\nu_t = C_\mu \frac{k^2}{\varepsilon}, \tag{5}$$

where $C_\mu = 0.09$ is a constant. The semi-empirical model transport equations for k and ε may be given as [1]

$$\frac{\partial k}{\partial t}+\frac{\partial (uk)}{\partial x}+\frac{\partial (vk)}{\partial y}=\frac{\partial}{\partial x}\left(\left(\nu+\frac{\nu_t}{\sigma_k}\right)\frac{\partial k}{\partial x}\right)+\frac{1}{y}\frac{\partial}{\partial y}\left(y\left(\nu+\frac{\nu_t}{\sigma_k}\right)\frac{\partial k}{\partial y}\right)+ \\ +P+G-\varepsilon+S_k, \tag{6}$$

and

$$\frac{\partial \varepsilon}{\partial t}+\frac{\partial (u\varepsilon)}{\partial x}+\frac{\partial (v\varepsilon)}{\partial y}=\frac{\partial}{\partial x}\left(\left(\nu+\frac{\nu_t}{\sigma_\varepsilon}\right)\frac{\partial \varepsilon}{\partial x}\right)+\frac{1}{y}\frac{\partial}{\partial y}\left(y\left(\nu+\frac{\nu_t}{\sigma_\varepsilon}\right)\frac{\partial \varepsilon}{\partial y}\right)+ \\ +C_1\frac{\varepsilon}{k}P-C_2\frac{\varepsilon^2}{k}+S_\varepsilon, \tag{7}$$

respectively, where

$$P=\nu_t\rho_w\left[2\left(\frac{\partial u}{\partial y}\right)^2+2\left(\frac{\partial v}{\partial x}\right)^2+2\left(\frac{u}{r}\right)^2+\left(\frac{\partial u}{\partial x}+\frac{\partial v}{\partial y}\right)^2\right] \tag{8}$$

is the generation of turbulent kinetic energy due to mean velocity gradients (due to shear, that is), and

$$G=-g\frac{\nu_t}{\sigma_t}\frac{\partial \rho}{\partial x} \tag{9}$$

corresponds to the generation of turbulent kinetic energy due to buoyancy, where $\sigma_t = 0.85$ is the turbulent Prandtl number. The sludge density, ρ, in eqn (9) is expressed in terms of the sludge concentration, X, using eqn (4). In eqns (6) and (7), $\sigma_k = 1.0$ and $\sigma_\varepsilon = 1.3$ are the turbulent Prandtl numbers for k and ε, respectively. In eqn (7), $C_1 = 1.44$ and $C_2 = 1.92$ are constants. For stably stratified flow, which prevails in secondary clarifiers and which tends to suppress turbulence ($G < 0$), the effect of buoyancy on the dissipation of turbulent kinetic energy may be neglected [1].

Two source terms, $S_k = -(q_{rec}/V_{rec})k$ and $S_\varepsilon = -(q_{rec}/V_{rec})\varepsilon$, appear in eqns (6) and (7), respectively, which we use to account for the effect of the sludge removal on the turbulence kinetic energy and its dissipation rate. Both S_k and S_ε, and also G, are built into the CFD code using UDFs.

4 Activated sludge rheology

We have used a rotational viscometer to carry out our on-site rheology experiments. These experiments have shown that at low strain rates, typical of the flow in secondary clarifiers, the activated sludge exhibits Casson-type non-Newtonian flow behaviour. At larger strain rates, Bingham-type flow behaviour was observed. Our observations agree well with those made by Dollet [4].

The Casson equation for the dynamic viscosity, μ, may be given as

$$\mu=\nu\rho_w=\left(\frac{K_1}{\dot{\gamma}^{1/2}}+K_2\right)^2, \tag{10}$$

where $\dot{\gamma}$ is the strain rate, K_1 is the Casson yield stress parameter, and K_2 is the Casson viscosity parameter. Our rheology experiments show that K_1 depends quadratically on the concentration,

$$K_1 = C_1 X^2 + C_2 X \,. \tag{11}$$

Our experiments suggest further that K_2 is independent of the concentration for $X \geq X^*$ = 2 kg m^{-3} and equal to the mean value, $\overline{K}_2$. For the water viscosity value, μ_w, to emerge correctly as $X \to 0$, K_2 is assumed to depend linearly on the concentration on the interval $0 < X < X^*$. Thus,

$$K_2 = \begin{cases} \overline{K}_2 & (X \geq X^*) \\ \mu_w^{1/2} + \dfrac{(\overline{K}_2 - \mu_w^{1/2})}{X^*} X & (0 < X < X^*) \end{cases}. \tag{12}$$

The values of the parameters in eqns (11) and (12) are given in table 1 for three different temperatures. During the experiments, which were conducted over three days in April 2005, the concentration was varied between 2.8 and 9.5 kg m^{-3} using dilution and decantation. The sludge samples were taken at the outlet of the aeration basin. We have repeated our rheology measurements in July 2005 and found that the rheological flow behaviour was unchanged. Eqns (10) to (12) are built into the CFD code using a UDF.

Table 1: Viscosity parameters in eqns (11) and (12) for varying temperatures, T. The temperature in the clarifier was 15°C in March and April, and 20°C in July.

T [°C]	$C_1 \left[\dfrac{\mathrm{m}^{11/2}}{\mathrm{kg}^{3/2}\,\mathrm{s}}\right]$	$C_2 \left[\dfrac{\mathrm{m}^{5/2}}{\mathrm{kg}^{1/2}\,\mathrm{s}}\right]$	$\overline{K}_2 \left[\dfrac{\mathrm{kg}^{1/2}}{\mathrm{m}^{1/2}\,\mathrm{s}^{1/2}}\right]$	$\mu_w^{1/2} \left[\dfrac{\mathrm{kg}^{1/2}}{\mathrm{m}^{1/2}\,\mathrm{s}^{1/2}}\right]$
10	0.00307	0.0187	0.0463	0.0362
15	0.00281	0.0176	0.0445	0.0341
20	0.00319	0.0146	0.0436	0.0361

5 Conservation of particulate mass and sludge settling

The concentration field in the clarifier is governed by a convection-diffusion equation, which may be given as [1]

$$\frac{\partial X}{\partial t} + \frac{\partial((u-u_s)X)}{\partial x} + \frac{\partial(vX)}{\partial y} = \frac{\partial}{\partial x}\left(\frac{\nu_t}{\sigma_s}\frac{\partial X}{\partial x}\right) + \frac{1}{y}\frac{\partial}{\partial y}\left(y\frac{\nu_t}{\sigma_s}\frac{\partial X}{\partial y}\right) + S_X \,, \tag{13}$$

where σ_s = 0.7 is the turbulent Schmidt number, $u_s = u_s(X)$ is the settling velocity function, and $S_X = -(q_{rec}/V_{rec})X$ is the sludge removal source term.

The settling velocity, u_s, is expressed in terms of the concentration, X, using the double-exponential function of Takács *et al*. [5],

$$u_s = u_{s0} \exp[-r_h (X - X_{ns})] - u_{s0} \exp[-r_p (X - X_{ns})] \,. \tag{14}$$

The maximum settling velocity, u_{s0}, and the parameter that describes hindered settling, r_h, were determined from settling experiments. The minimum sludge

concentration, X_{ns}, describes the concentration of non-settleable solids in the effluent, and its value has been measured by decantation. The parameter that describes particulate settling at low sludge concentrations, r_p, is obtained from a fit of eqn (14) to the experimental settling data. It is generally an order of magnitude larger than r_h [6].

From our settling experiments, we found values for u_{s0} that vary between 0.89 and 1.22 mm s^{-1}, and for r_h that vary between 0.225 and 0.284 m^3 kg^{-1}. The value for X_{ns} was found to be 5.2×10^{-3} kg m^{-3}, and we have used a value of 2.5 m^3 kg^{-1} for r_p. The on-site settling experiments were conducted in March and April 2005, and in July 2005. The results of these settling velocity measurements agree well with literature data [6].

We have added eqn (13), including the settling velocity function, eqn (14), the sludge removal source term, S_X, and the turbulent dispersion coefficient, ν_t/σ_s, to the CFD code as a user-defined scalar equation in Fluent using UDFs.

6 Computational domain and sludge removal zone

The clarifier has a depth of 3 m everywhere and a diameter of about 33 m. Settled sludge is removed from the bottom region of the clarifier by means of suction-lift through an array of six suction pipes. These pipes are situated underneath the slowly rotating clarifier bridge and remove sludge locally in the near-bottom region underneath the bridge. The suction-lift sludge withdrawal mechanism thus disturbs the otherwise axisymmetric geometry of the clarifier. To reduce computational efforts, we have abstracted the sludge withdrawal mechanism with a disk-like sludge removal zone in the near-bottom region of the clarifier in our axisymmetric CFD model. In the CFD model, sludge is thus removed everywhere in the near-bottom region of the clarifier.

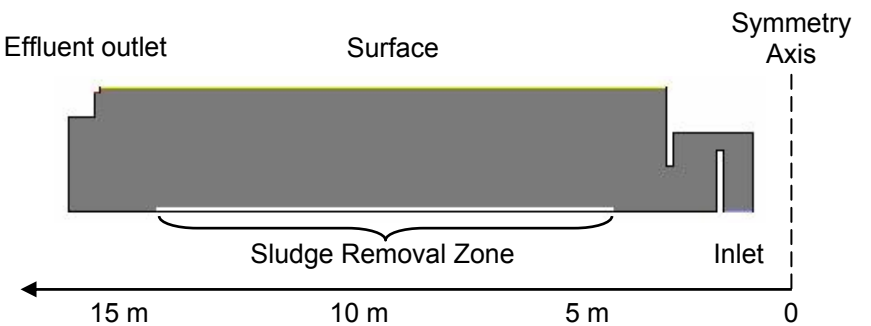

Figure 2: Computational domain and boundaries of the clarifier model.

The computational domain is shown in fig. 2, where the disk-like sludge removal zone in the near-bottom region of the clarifier is indicated (in white). The volume of the sludge removal zone, V_{rec}, can be calculated using

$$V_{rec} = \pi(R_o^2 - R_i^2)h \,. \tag{15}$$

with an inner radius of R_i = 3.7 m, an outer radius of R_o = 14.7 m, and a height of h = 0.15 m from the clarifier bottom, the volume of the sludge removal zone is V_{rec} = 2.86 m^3. The height of the sludge removal zone corresponds to the lower end of the suction pipes, and the distance $R_o - R_i$ = 11.0 m is the length of the array of suction pipes underneath the bridge.

7 Boundary conditions

At the clarifier inlet, we apply the measured inlet concentration, X_{in}, and the inlet velocity components, u_{in} and v_{in}. The axial component of the inlet velocity is determined from the measured flow rate, Q_{in}, and the cross-sectional area,

$$u_{in} = \frac{Q_{in}}{\pi(R_{a,o}^2 - R_{a,i}^2)}, \tag{16}$$

where $R_{a,o}$ and $R_{a,i}$ are the outer and the inner radius of the inlet annulus, respectively, and Q_{in} is the flow rate at the clarifier inlet. The radial component of the inlet velocity is zero, $v_{in} = 0$.

The turbulent kinetic energy at the inlet, k_{in}, is calculated using

$$k_{in} = 1.5 \times (I_u u_{in})^2, \tag{17}$$

where $I_u = 0.05^2$ is the turbulence intensity [1]. Its dissipation rate at the inlet, ε_{in}, is obtained from

$$\varepsilon_{in} = \frac{C_\mu^{3/4} k_{in}^{3/2}}{\kappa L_u}, \tag{18}$$

in which $\kappa = 0.4$ is the von Kármán constant. The turbulence length scale, L_u, is estimated using the recommendations of Lakehal *et al*. [1].

The movement of the free surface is neglected. The axial velocity component is set to zero at the surface, and the radial velocity component is computed assuming full slip. The gradient of the radial velocity and the gradients of all scalar variables normal to the surface are set to zero.

At the effluent outlet boundary, the values of the variables are extrapolated from computed near-outlet values, so that the streamwise gradients are zero.

The no-slip condition must be obeyed at all solid boundaries. The concentration gradients perpendicular to all solid walls are zero. We use logarithmic wall functions to model the turbulent flow in the near-wall region.

8 Computed results and comparison with measurements

The computed velocity field and sludge distribution is shown in figs. 3 and 4, respectively. We note that the steady-state conditions were computed using a time-marching procedure to facilitate convergence. The difference in density between incoming mixed liquor and clear water in the inlet region of the clarifier directs the flow downwards before the sludge mixture spreads out into the clarifier. Fig. 3 shows that the main flow is directed along the upper limit of the sludge blanket before leaving the clarifier through the effluent outlet. The concentration field in fig. 4 shows the layered structure of the sludge blanket.

Figure 3: Velocity field in units of [m s^{-1}] in the clarifier for 7 July 2005 (X_{in} = 4.93 kg m^{-3}, q_{rec} = 100.4 kg s^{-1}, u_{in} = 0.065 m s^{-1}).

Figure 4: Concentration field in units of [kg m^{-3}] in the clarifier for 7 July 2005 (X_{in} = 4.93 kg m^{-3}, q_{rec} = 100.4 kg s^{-1}, u_{in} = 0.065 m s^{-1}).

The comparison of measured and computed concentration profiles in figs. 5 and 6 show that the model predicts the sludge distribution in the inlet region well. At longer radial distances from the centre of the clarifier, the model underpredicts and overpredicts the height of the sludge blanket for the data of March and July, respectively. Unequal sludge withdrawal through the suction pipes or dynamic flow conditions during the measurements may be the cause of these discrepancies. The concentration values that were measured near the clarifier bottom in July are not reproduced by the CFD model (fig. 6). However, the average concentration value in the sludge removal zone computed by the CFD model (9.04 kg m^{-3}) compares very well to the value that was measured in the recycle stream (9.71 kg m^{-3}). The computed effluent concentrations for March and July are nearly equal, at 10.7 and 12.9 g m^{-3}, respectively, which agrees well with our measured effluent concentration values (6 to 16 g m^{-3} for all our measurements).

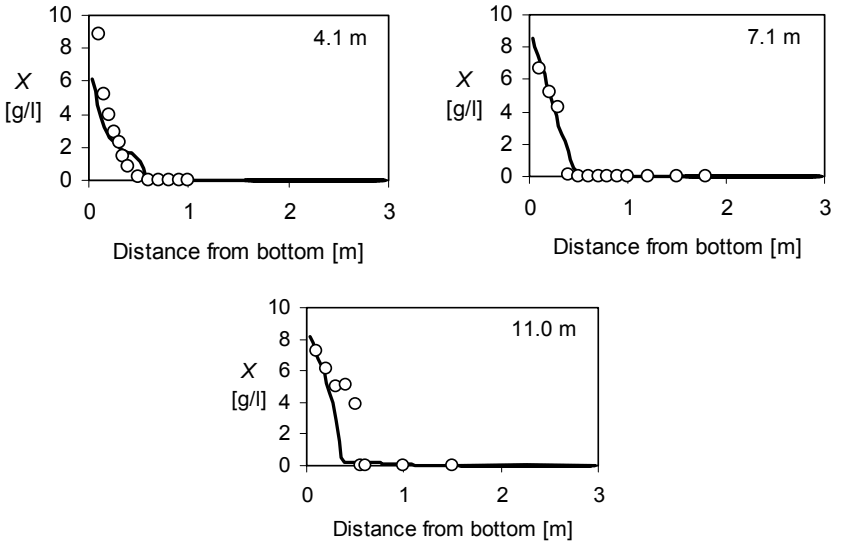

Figure 5: Computed (lines) and measured (symbols) concentration profiles in the clarifier at varying radial distances from the clarifier centre for 31 March 2005 (X_{in} = 3.91 kg m^{-3}, q_{rec} = 75.7 kg s^{-1}, u_{in} = 0.049 m s^{-1}).

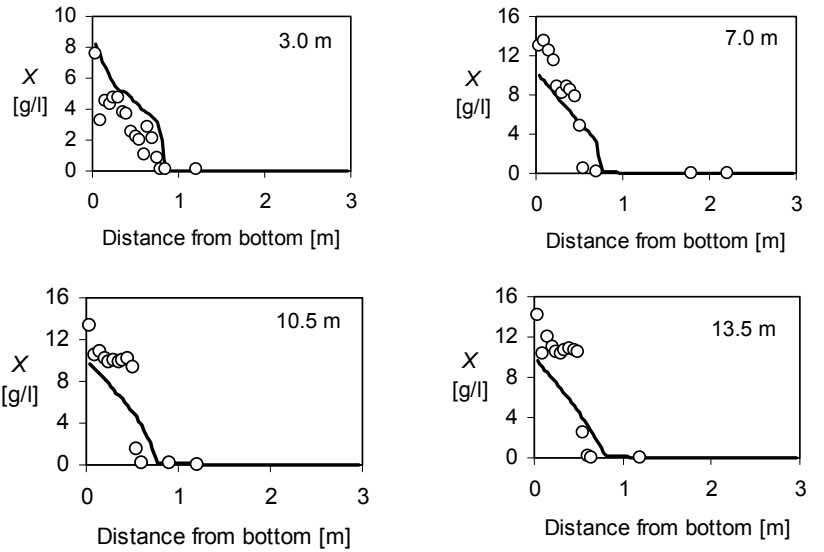

Figure 6: Computed (lines) and measured (symbols) concentration profiles in the clarifier at varying radial distances from the clarifier centre for 7 July 2005 (X_{in} = 4.93 kg m^{-3}, q_{rec} = 100.4 kg s^{-1}, u_{in} = 0.065 m s^{-1}).

9 Conclusions

We have developed an axisymmetric CFD model within the CFD code Fluent 6 that predicts the sedimentation of activated sludge in secondary clarifiers. On-site measurements were carried out at the wastewater treatment plant of Saint Malo (France), where the clarifiers are equipped with suction-lift sludge removal systems. The model employs negative source terms in the governing field equations to simulate this sludge withdrawal mechanism. These source terms remove the sludge within a sludge removal zone adjacent to the clarifier bottom. Sludge rheology measurements showed that the flow behaviour in the clarifier is well described using the Casson viscosity model. Settling experiments provided the parameters for the double-exponential settling velocity function. The computed sludge distribution compares well with measured concentration profiles in the inlet region of the clarifier. At larger distances from the clarifier centre, the prediction of the sludge blanket height is less good, which may be caused by unequal sludge withdrawal and dynamic flow conditions during the measurements. The concentrations in the recirculation stream and in the effluent outlet are well predicted by the CFD model.

Acknowledgement

M. Weiss and B. Gy. Plosz gratefully acknowledge financial support from the European Commission for two industry-host Marie Curie post-doctoral research fellowships.

References

[1] Lakehal, D., Krebs, P., Krijgsman, J. & Rodi, W., Computing Shear Flow and Sludge Blanket in Secondary Clarifiers. *Journal of Hydraulic Engineering*, pp. 253 – 262, March 1999.

[2] Dahl, C., Numerical Modelling of Flow and Settling in Secondary Settling Tanks. *PhD Thesis*, Aalborg University, Denmark, 1993.

[3] Nopens, I., Modelling the Activated Sludge Flocculation Process: A Population Balance Approach. *PhD Thesis*, University of Gent, Belgium, 2005.

[4] Dollet, P., Characterisation of the State of Flocculation of Activated Sludge Using Rheological Measurements (in French), *PhD Thesis*, University of Limoges, France, 2000.

[5] Takács, I., Patry, G.G. & Nolasco, D., A Dynamic Model of the Clarification-Thickening Process. *Water Research*, **25(10)**, pp. 1263 – 1271, 1991.

[6] Ekama, G.A., Barnard, J.L., Günthert, F.W., Krebs, P., McCorquodale, J.A., Parker, D.S. & Wahlberg, E.J., *Secondary Settling Tanks: Theory, Modelling, Design and Operation*. IAWQ: London, 1997.